Matter and Radiation at Extremes | RESEARCH ARTICLE | scitation.org/journal/mre

A semi-classical model for the charge exchange and energy loss of slow highly charged ions in ultrathin materials

Cite as: Matter Radiat. Extremes 4, 054401 (2019); doi: 10.1063/1.5110931
Submitted: 21 May 2019 • Accepted: 10 June 2019 •
Published Online: 29 July 2019

Xun Guo,[1,a] Yanjun Fu,[1,a] Xitong Zhang,[1,2] Xinwei Wang,[3] Yan Chen,[4] and Jianming Xue[1,2,b]

AFFILIATIONS

[1]State Key Laboratory of Nuclear Physics and Technology, School of Physics, Peking University, Beijing 100871, People's Republic of China
[2]CAPT, HEDPS and IFSA Collaborative Innovation Center of MoE, College of Engineering, Peking University, Beijing 100871, People's Republic of China
[3]School of Advanced Materials, Shenzhen Graduate School, Peking University, Shenzhen 518055, People's Republic of China
[4]New Energy Research Institute, School of Environment and Energy, South China University of Technology, Guangzhou 510006, People's Republic of China

[a]**Contributions:** X. Guo and Y. Fu contributed equally to this work.
[b]**Electronic mail:** jmxue@pku.edu.cn

ABSTRACT

We present a simple and reliable method, based on the over-barrier model and Lindhard's formula, to calculate the energy loss, charge transfer, and normalized intensity of highly charged ions penetrating through 2D ultrathin materials, including graphene and carbon nanomembranes. According to our results, the interaction between the ions and the 2D material can be simplified as an equivalent two-body collision, and we find that full consideration of the charge exchange effect is key to understanding the mechanism of ion energy deposition in an ultrathin target. Not only can this semiclassical model be used to evaluate the ion irradiation effect to a very good level of accuracy, but it also provides important guidance for tailoring the properties of 2D materials using ion beams.

I. INTRODUCTION

Ultrathin materials, including polymeric membranes, graphene, and carbon oxide monolayers, play an important role in ion/molecule separation technology, water treatment, and the chemical industry.[1,2] In particular, microstructures on such ultrathin materials, such as vacancies, nanoholes, and boundaries, generated by the ion beam technique, which has long been used as a powerful modification tool,[3–5] can significantly influence their ion/molecule transport properties and selectivity.[6,7]

Recently, a particular category of energetic ions, namely, slow highly charged ions (HCIs), has received much attention for tailoring the properties of nanomaterials,[8–10] especially 2D ultrathin materials such as graphene and carbon nanomembranes (CNMs).[11–13] The energy deposition from these ions can be confined within a shallow region beneath the surface of the nanomaterial,[14] which makes the technique very promising for fabrication of nanoscale devices.[15,16] The mechanism of the interaction between incident ions and the target ultrathin material is therefore of crucial importance, and a theoretical calculation model is also urgently needed to facilitate further development of the HCI technique.

Unlike low-charge-state energetic ions, which deposit energy into a target material mainly via nuclear and electronic energy loss processes during collisions,[14,17] HCIs can also deposit their energy via a charge exchange process, by capturing electrons from the target.[18,19] For most 3D materials, this charge exchange process occurs only in the first few collisions of the incident ions with the topmost few layers of target atoms; for example, with Xe ions with energy in the range 3.6–400 keV, the depth for charge transfer is only about 1–4 nm, which is much less than the total range of the energetic ions (about 6–90 nm).[20] These collisions can quickly reduce the charge state of an incident ion to an equilibrated low-charge state: $Q_{eq} = Z^{1/3}v/v_0$, where Z and v are the nuclear charge and velocity of the incident ion,

respectively, and v_0 is the Bohr velocity, according to Bohr's stripping criterion.[21]

However, when energetic ions penetrate through an ultrathin material (with, e.g., thickness <1 nm), since such a material is composed of only a few layers of atoms, only a very small number of atoms will be involved in this interaction, certainly not enough to fully equilibrate the ion charge state,[22–24] so the value of the charge exchange cannot be estimated simply as $Q_{in}-Q_{eq}$ (where Q_{in} is the original charge state of the incident ion), and therefore its evaluation should be treated with great care.[18,20] According to previous experimental studies, there is a dependence between charge exchange and energy loss of the incident ions, for example, for Xe ions penetrating through graphene monolayers[25] and CNMs.[23] It has also been confirmed that a higher-charge state results in a greater energy loss for the incident ion, and the energy loss would be greatly underestimated if the charge state were treated as equilibrated during the calculation.[23]

Unfortunately, the relation between charge exchange and the electronic energy loss process is still unclear,[14,19,26] so an appropriate calculation model that can precisely describe these interactions is urgently needed, both for further improvements in modification technology and for evaluation of radiation resistance. In this paper, we develop a new semiclassical model, which is based on the Lindhard formula[14,27] and the over-barrier model (OBM)[28–30] for the electronic energy loss and charge exchange processes. This model is able to give a quantitative explanation of experimental results to a very good level of accuracy.

Our model can be summarized as follows. When an ion interacts with ultrathin material, the interaction can be divided into three parts: nuclear energy loss, electronic energy loss, and charge exchange. According to our calculations, the influence of nuclear energy loss can be ignored if we focus only on small-angle scattering, as discussed in the supplementary material. Besides, electronic energy loss and charge exchange are treated as two independent processes in our model, and we have found that with this treatment, the problem can be solved with a good accuracy compared with the experimental results, which implies that the application of this approach is reasonable for the given conditions. Moreover, the interaction between an incident ion and target atoms can be approximated as the interaction of the ion with a single equivalent atom, because in an ultrathin material, only a few target atoms at most, possibly only one, can be involved in the interaction. We called this an equivalent atom because it can provide a far greater number of electrons than it actually possesses. This treatment simplifies the many-body interaction as an equivalent binary collision, which is an approach that is also widely used in similar studies.[31]

II. METHOD

To calculate the charge exchange between the incident ion and ultrathin material, we extend the semiclassical OBM method,[28] which was previously developed for the one-optional-electron and two-body interaction problem[28–30,32,33] When an energetic ion (**P**) with velocity v approaches a target atom (**T**) within a distance R and with an impact parameter d, the electrons of **T** will have a probability of P to climb over the potential barrier and be captured by **P**, as shown in Fig. 1. In the following, all the units are atomic units unless otherwise specified.

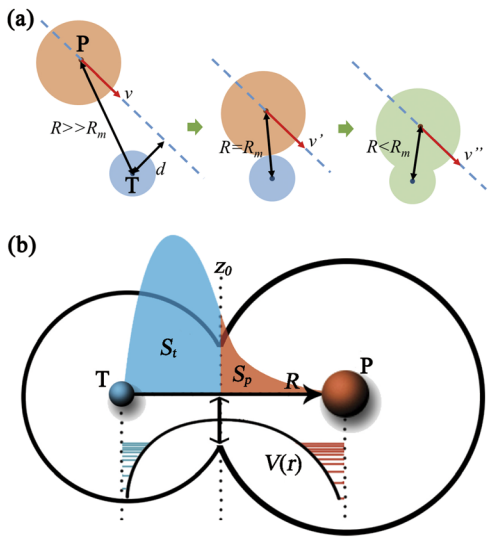

FIG. 1. Geometry of scattering. (a) When an energetic ion **P** with velocity v and impact parameter d moves toward the target **T**, their electron clouds start to overlap (green area) when $R < R_m$. (b) The enveloping curve shows a section of the equipotential surface at a given distance R between **P** and **T**. This curve represents the border of the classically accessible region for the electrons. S_t and S_p are the areas of the electron density distribution function separated by the potential saddle point at z_0. $V(r)$ is the potential function between **T** and **P**. The probability of electron transfer to **P** at time t is $N_\Omega(t) = S_p(t)/[S_t(t) + S_p(t)]$.

Similar to the classical OBM model, it is the opening of the equipotential curve between **T** and **P** that leads to a leakage of electrons from **T** to **P**, and the distance R_m at which the opening vanishes can be written as follows:[28–30]

$$R_m = \frac{\alpha\sqrt{Z_p Z_t} + Z_t}{E_n}, \tag{1}$$

where Z_t and Z_p are the charges of **P** and **T**, respectively, α is an adjustable parameter to gauge the influence of different incident charge states,[28–30] and E_n is the orbital energy. According to Sattin,[30] $\alpha = 1$ or 2 gave the best agreement with experiment, which suggests that the perturbation of the electron trajectory of the target by the incident ion can be neglected.

The probability P for capturing an electron is given by[28–30]

$$P = 1 - \exp\left[-\frac{f_T}{T_{em}}\int_{-\infty}^{+\infty} N_\Omega(t)\,dt\right], \tag{2}$$

where $T_{em} = 2\pi/Z_t^3$ is the period of the electron orbital motion, f_T is a parameter for correcting T_{em} by taking into account the perturbation by the projectile,[29,30] and $N_\Omega = \int_{z_0}^{\infty}\rho(r)\,dr$, where $\rho(r)$ is the electron density radial distribution function. It should be noted that the traditional OBM model treats only a single-electron process for the ion/isolated-atom interaction, so it uses a single-electron distribution function for $\rho(r)$. However, the actual charge exchange process for an ion involves multiple electrons, and therefore we use the total-electron density distribution function instead for the entire calculation.

In addition, the maximum number of electrons transferred to an ion, ΔQ_{max}, can be much greater than the atomic number of the target atoms, because the valence electrons in ultrathin material are delocalized, and the depletion of electrons due to charge transfer can be quickly replenished from neighboring atoms in a very short time.[23] Therefore, we can safely assume that the electron density distribution $\rho(r)$ is quasi-constant in time [i.e., $\rho(r)$ does not change significantly within an interval Δt, but it can take different values in different integration steps] over the entire charge exchange process, and the integration over $N_\Omega(t)\,dt$ can be calculated as the sum $\sum_{i=1}^{M} N_\Omega(t_i)\Delta t$. In this study, the total integral length was divided into $M = 5000$ steps, and the maximum distance between **T** and **P** was more than 30 Å.

The probability P at different impact parameters d can be calculated using Eq. (2). Assuming that when $d = d_{min}$, the exchanged charge reaches a maximum value ΔQ_{max} with probability P_{max}, the exchanged charge ΔQ for arbitrary d can be obtained as

$$\Delta Q(d) = \Delta Q_{max}\frac{P(d)}{P_{max}}.$$

For the electronic energy loss, we use the method developed by Lindhard, where the force on a projectile is obtained from the change in the electron density distribution induced by the electric field of the projectile.[14,34] The response of the electron density is obtained from the dielectric constant $\epsilon(k, \omega)$, which is a function of frequency ω and wave vector k. Therefore, the electronic energy loss can be described as[14]

$$\frac{dE}{dx} = -\frac{2Z_p^2 e^2}{\pi v^2}\int_0^{kv}\omega\, d\omega \int_0^{\infty}\frac{dk}{k}\,\mathrm{Im}\left\{\frac{1}{\epsilon(k,\omega)}\right\}. \quad (3)$$

Note that the charge state Z_p in the conventional description is defined as its value in the equilibrium charge state. However, in this case, the ion charge state is far from equilibrium, and, in fact, it should be fairly close to its original state if the material is thin enough. Therefore, we simply approximate $Z_p = Q_{in}$ in Eq. (3) to calculate the total electronic energy loss ΔE for every value of d. A more detailed discussion of Lindhard's energy loss formula can be found in the second section of the supplementary material.

III. RESULTS AND DISCUSSION

To test our model, we used it to interpret a number of experimental results that were obtained over a period of nearly 10 years, but previously lacked a theoretical explanation.[22,23] In these experiments, Xe^{q+} ions were used to penetrate a 1 nm-thick CNM, and ejected ions with small emergent angle (<1.6°) were detected. According to our calculations, d_{min} should be larger than 1 a.u. to obtain an emergent angle less than 1.6°, and d at such a value is large enough that the nuclear energy loss can be neglected, which is also consistent with the conclusions of a previous study.[23] Therefore, in the calculation described below, d_{min} was set as 1 a.u., and the nuclear energy loss was not taken into account. A detailed discussion of the evaluation of d_{min} can be found in the first section of the supplementary material.

A. d–ΔQ and d–ΔE relationships

The charge exchange probabilities were first calculated for various d, and $\rho(r)$ of an isolated carbon atom was calculated using a density functional theory (DFT) method.[35,36] According to our calculation, the average ionization energy for the outer four electrons of carbon is about 37 eV, and this value was used for E_n. In addition, the contributions from the inner electrons were negligible and were therefore neglected in the calculation.

To reconcile our calculations with the experimental results,[23] $\Delta Q_{max} = Z_p - 2$ was assumed when $d = d_{min} = 1.00$ a.u., and, for an arbitrary d, $\Delta Q(d) = (Q_{in} - 2)P(d)/P(1\text{ a.u.})$. By assuming $f_T = 10$, the d–ΔQ relationship was calculated, with the results shown in Fig. 2(a), from which it can be seen that a higher Q_{in} will lead to a greater ΔQ for ions. The corresponding d–ΔE relationship was calculated using Eq. (3) with the previously obtained electron density distribution, with the results shown in Fig. 2(b). A detailed discussion of the setting of α and f_T can be found in the first section of the supplementary material.

B. Comparison with experimental results

By linking ΔQ and ΔE via the impact parameter d, the relationship between them for each Q_{in} can be calculated, and the results are plotted as open squares in Fig. 3(a), where experimental data (points with error bars) are also illustrated. Experimental data and

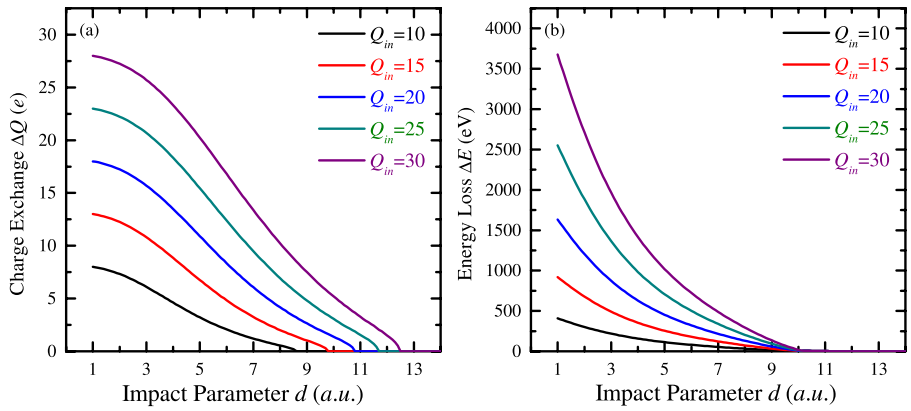

FIG. 2. (a) Charge exchange ΔQ and (b) electronic energy loss ΔE at different impact parameters d, with $\alpha = 1$, $f_T = 10$, $d_{min} = 1.00$ a.u., and $\Delta Q_{max} = 18e^-$.

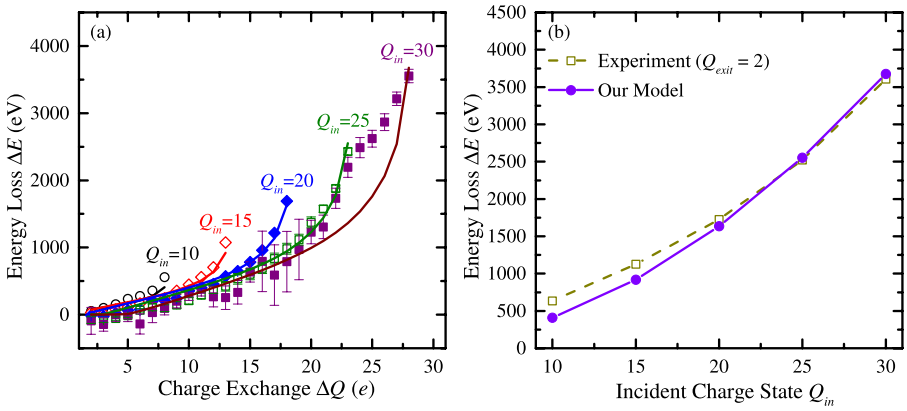

FIG. 3. (a) Energy loss ΔE of 40 keV Xe^{q+} ions in CNM as a function of charge exchange ΔQ. Points and lines represent experimental data[23] and calculated values, respectively. (b) Relation between ΔE and incident charge state Q_{in} for $Q_{exit} = 2$. Open squares represent experimental data[23] and solid squares are calculated from the values in (a).

calculated values for ΔE as a function of Q_{in} when the exit charge state $Q_{exit} = 2$ are shown in Fig. 3(b).

As can be seen from Fig. 3, the calculated values match the experimental data better at higher Q_{in} and lower ΔQ. For very high-charge states, in particular $Q_{in} = 30$ with very large ΔQ, a small deviation is present, which can be ascribed to some unidentified secondary effects, such as structural change induced by potential energy deposition. Meanwhile, charge exchange still occurs at very large d, and, in this case, the defects in the thin CNM, such as nanoholes and cracks, may allow the ion to interact with carbon atoms at a greater distance, resulting in fewer transferred charges.

C. Normalized intensity of different Q_{exit}

Our model can also be applied to calculate the intensity of each Q_{exit} for CNMs. The CNMs under investigation were not atomically homogeneous and contained many microholes as a result of their fabrication from a self-assembled monolayer of 1,1′-biphenyl-4-thiol $[H(C_6H_4)_2\text{-}SH]$ via low-energy electron irradiation to crosslink the molecules and remove the hydrogen atoms.[12] We therefore separated the carbon atoms into two types for the calculation, namely, those inside the molecular clusters and those on the periphery of the clusters. The average contribution of two types of atoms can be represented by a parameter β reflecting the percentage of each atom type. A detailed calculational treatment of the target can be found in the third section of the supplementary material.

The calculated relations between the intensities and Q_{exit} for five different values of Q_{in} are plotted in Fig. 4. Experimental data points with error bars are adapted from a previous publication[23] for comparison, and the calculated intensities are all normalized by setting the first point of each curve equal to the corresponding experimental value. Excellent agreement between the calculated and experimental values can be seen. Moreover, according to our calculations, the value of β changed when $Q_{in} \geqslant 25$, which means that the atomic structure of the target CNM was obviously changed by incident ions with kinetic energy equal to 40 keV. This conclusion is also consistent with the results of Ritter *et al.*[37]

These agreements demonstrate that our model is able to accurately describe the process of interaction that occurs when ions penetrate a CNM. On the other hand, although the experimental data showed an apparent dependence of ΔE on ΔQ, this does not fundamentally represent a direct influence of charge exchange on electronic energy loss. In a binary collision problem, ΔE and ΔQ are linked via d, since both ΔE and ΔQ depend on the impact parameter. However, if we extend this method to the investigation of many-body collisions, d loses its original physical meaning and can be viewed as an equivalent parameter.

D. ΔQ–ΔE relation in a graphene monolayer

To further show the general applicability of our model, we also applied it to calculate the case of Xe^{q+} ions interacting with a graphene monolayer. Similarly to the approach adopted in the CNM case, we calculated the ΔQ–ΔE relation for graphene with the same parameters, as shown in Fig. 5. As can be seen, there are now some differences between the simulation and experimental results, with the relative difference being as high as 30% for a high incident charge state. For low Q_{in}, the relative difference is no more than 10%, which

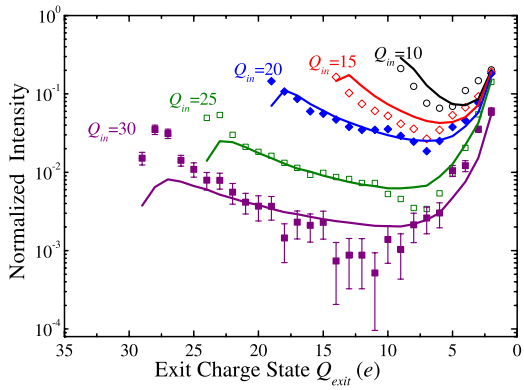

FIG. 4. Normalized intensities of exit charge states Q_{exit} for different incident charge states Q_{in}. Points and lines represent experimental data[23] and calculated values, respectively.

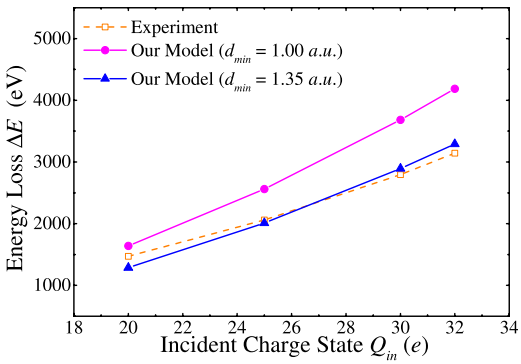

FIG. 5. Comparison of calculated and experimentally measured[25] ΔE–ΔQ relations for 40 keV Xe^{q+} ions penetrating through a graphene monolayer (when $Q_{exit} = 2$). The calculation represented by the pink dots used the same parameters as for the CNM calculation, while for the calculation represented by the blue triangles, d_{min} was adjusted to 1.35 a.u., which gives better agreement with the experimental values.

means that the model can still give a good prediction in this case. So far, we have not been able to give a reasonable explanation for this phenomenon.

However, as can also be seen in Fig. 5, if we increase d_{min} to 1.35 a.u., the calculated ΔQ–ΔE relation is in excellent agreement with the experimental results. As discussed previously, d_{min} represents the maximum emergent angle: a higher d_{min} means a lower maximum emergent angle (d_{min} = 1.35 a.u., which corresponds to 0.8°–1.1°). We therefore predicted that it might be more difficult for large-angle scattering to occur in graphene than in a CNM.

Thus, the model presented here is applicable to both CNM and graphene, although only a simple binary collision approximation is employed. In addition to corroborating our assumption that only a few target atoms participate in the interaction, these results also imply that the timescale for the charge exchange between the projectile and the target atom is much longer than that for electron replenishment from nearby atoms, since the electronic response in these kinds of low-dimensional materials is very fast.[25] Besides, as we previously assumed, all the electrons are simultaneously transferred to the projectile atom; this assumption might be somewhat counter-intuitive because the inner orbitals may not be enough to accommodate all the transferred electrons at the same time. A possible explanation is that the electrons perhaps first transfer into the outer orbitals, and then fall into the inner orbitals after the interaction.

It should also be noted that although we neglected the contributions from the inner electrons of carbon in the above calculations, these contributions could, technically, also be included. In fact, as with our previous assumption, it makes no difference whether we include these inner electrons or not. However, if the energy of the ions is further increased, the probability of transferring the inner electrons will also increase, and it may become non-negligible at some stage. Only in this case should we include the inner electrons in the calculation, and our model would then still be applicable for higher-energy ions.

IV. CONCLUSIONS

In summary, we have developed a new semiclassical model based on the OBM and Lindhard's formula to describe the interactions between ions and ultrathin materials, including graphene and CNMs. We have found that the processes of charge exchange and energy loss can be treated independently, and their apparent correlation can be linked via the impact parameter. Our model is able to accurately describe the experimentally measured ΔQ–ΔE relation for various incident ions and predict the intensity of ejected ions with different charge states. This model should be of great importance for fundamentally understanding the novel physical phenomena related to ion interactions with carbon-based ultrathin materials, and it could also be applied to other kinds of 2D materials.

SUPPLEMENTARY MATERIAL

See the supplementary material for a specific evaluation of the values of α, f_T, and d_{min}, and for more details about Lindhard's formula, including the exact expression for $\epsilon(k, \omega)$, and the derivation of the normalized intensity of ejected ions.

ACKNOWLEDGMENTS

This work is financially supported by the NSFC (Grant No. 11705010), the NSAF (Grant No. U1230111), the IAEA (CRP No. F11020 and Contract No. 21063), and the China Postdoctoral Science Foundation (Grant No. 2019M650351). The calculations were performed on the Weiming No. 1 and Life Science No. 1 High Performance Computing Platform at Peking University, as well as TianHe-1(A) at the National Supercomputer Center in Tianjin.

REFERENCES

[1]C. A. Amadei and C. D. Vecitis, "How to increase the signal-to-noise ratio of graphene oxide membrane research," J. Phys. Chem. Lett. **7**, 3791–3797 (2016).
[2]J. Schrier, "Helium separation using porous graphene membranes," J. Phys. Chem. Lett. **1**, 2284–2287 (2010).
[3]D. W. Boukhvalov and M. I. Katsnelson, "Chemical functionalization of graphene with defects," Nano Lett. **8**, 4374–4379 (2008).
[4]E. H. Åhlgren, J. Kotakoski, and A. V. Krasheninnikov, "Atomistic simulations of the implantation of low-energy boron and nitrogen ions into graphene," Phys. Rev. B **83**, 115424-1–115424-7 (2011).
[5]W. Li, X. Wang, X. Zhang, S. Zhao, H. Duan, and J. Xue, "Mechanism of the defect formation in supported graphene by energetic heavy ion irradiation: The substrate effect," Sci. Rep. **5**, 9935-1–9935-6 (2015).
[6]A. W. Hauser and P. Schwerdtfeger, "Nanoporous graphene membranes for efficient ^{3}He/^{4}He separation," J. Phys. Chem. Lett. **3**, 209–213 (2012).
[7]L. Huang, M. Zhang, C. Li, and G. Shi, "Graphene-based membranes for molecular separation," J. Phys. Chem. Lett. **6**, 2806–2815 (2015).
[8]R. Heller, S. Facsko, R. A. Wilhelm, and W. Möller, "Defect mediated desorption of the KBr(001) surface induced by single highly charged ion impact," Phys. Rev. Lett. **101**, 096102-1–096102-4 (2008).
[9]F. Aumayr, A. S. El-Said, and W. Meissl, "Nano-sized surface modifications induced by the impact of slow highly charged ions—A first review," Nucl. Instrum. Methods Phys. Res., Sect. B **266**, 2729–2735 (2008).
[10]F. Aumayr, S. Facsko, A. S. El-Said, C. Trautmann, and M. Schleberger, "Single ion induced surface nanostructures: A comparison between slow highly charged and swift heavy ions," J. Phys.: Condens. Matter **23**, 393001-1–393001-23 (2011).
[11]A. Turchanin, A. Beyer, C. T. Nottbohm, X. Zhang, R. Stosch, A. Sologubenko, J. Mayer, P. Hinze, T. Weimann, and A. Gölzhäuser, "One nanometer thin carbon nanosheets with tunable conductivity and stiffness," Adv. Mater. **21**, 1233–1237 (2009).
[12]A. Turchanin and A. Gölzhäuser, "Carbon nanomembranes from self-assembled monolayers: Functional surfaces without bulk," Prog. Surf. Sci. **87**, 108–162 (2012).

[13]U. Bangert, W. Pierce, D. M. Kepaptsoglou, Q. Ramasse, R. Zan, M. H. Gass, J. A. Van den Berg, C. B. Boothroyd, J. Amani, and H. Hofsäss, "Ion implantation of graphene-toward ic compatible technologies," Nano Lett. **13**, 4902–4907 (2013).
[14]C. P. Race, D. R. Mason, M. W. Finnis, W. M. C. Foulkes, A. P. Horsfield, and A. P. Sutton, "The treatment of electronic excitations in atomistic models of radiation damage in metals," Rep. Prog. Phys. **73**, 116501-1–116501-40 (2010).
[15]A. K. Geim, "Graphene: Status and prospects," Science **324**, 1530–1534 (2009).
[16]B. Guo, Q. Liu, E. Chen, H. Zhu, L. Fang, and J. R. Gong, "Controllable *n*-doping of graphene," Nano Lett. **10**, 4975–4980 (2010).
[17]D. Kost, S. Facsko, W. Möller, R. Hellhammer, and N. Stolterfoht, "Channels of potential energy dissipation during multiply charged argon-ion bombardment of copper," Phys. Rev. Lett. **98**, 225503-1–225503-4 (2007).
[18]F. Aumayr and H. Winter, "Slow highly charged ions -a new tool for surface nanostructuring," e-J. Surf. Sci. Nanotech. **1**, 171–174 (2003).
[19]R. A. Wilhelm, A. S. El-Said, F. Krok, R. Heller, E. Gruber, F. Aumayr, and S. Facsko, "Highly charged ion induced nanostructures at surfaces by strong electronic excitations," Prog. Surf. Sci. **90**, 377–395 (2015).
[20]A. S. El-Said, R. Heller, W. Meissl, R. Ritter, S. Facsko, C. Lemell, B. Solleder, I. C. Gebeshuber, G. Betz, M. Toulemonde, W. Möller, J. Burgdörfer, and F. Aumayr, "Creation of nanohillocks on CaF_2 surfaces by single slow highly charged ions," Phys. Rev. Lett. **100**, 237601-1–237601-4 (2008).
[21]W. Brandt and M. Kitagawa, "Effective stopping-power charges of swift ions in condensed matter," Phys. Rev. B **25**, 5631–5637 (1982).
[22]T. Schenkel, M. A. Briere, A. V. Barnes, A. V. Hamza, K. Bethge, H. Schmidt-Böcking, and D. H. Schneider, "Charge state dependent energy loss of slow heavy ions in solids," Phys. Rev. Lett. **79**, 2030–2033 (1997).
[23]R. A. Wilhelm, E. Gruber, R. Ritter, R. Heller, S. Facsko, and F. Aumayr, "Charge exchange and energy loss of slow highly charged ions in 1 nm thick carbon nanomembranes," Phys. Rev. Lett. **112**, 153201-1–153201-5 (2014).
[24]R. A. Wilhelm, E. Gruber, V. Smejkal, S. Facsko, and F. Aumayr, "Charge-state-dependent energy loss of slow ions. I. Experimental results on the transmission of highly charged ions," Phys. Rev. A **93**, 052708-1–052708-4 (2016).
[25]E. Gruber, R. A. Wilhelm, R. Pétuya, V. Smejkal, R. Kozubek, A. Hierzenberger, B. C. Bayer, I. Aldazabal, A. K. Kazansky, F. Libisch, A. V. Krasheninnikov, M. Schleberger, S. Facsko, A. G. Borisov, A. Arnau, and F. Aumayr, "Ultrafast electronic response of graphene to a strong and localized electric field," Nat. Commun. **7**, 13948-1–13948-7 (2016).
[26]G. Schiwietz and P. L. Grande, "Introducing electron capture into the unitary-convolution-approximation energy-loss theory at low velocities," Phys. Rev. A **84**, 052703-1–052703-7 (2011).
[27]J. Lindhard, "On the properties of a gas of charged particles," Dan. Vid. Selsk Mat.-Fys. Medd. **28**(8), 41–43 (1954), available at http://gymarkiv.sdu.dk/MFM/kdvs/mfm%2020-29/mfm-28-8.pdf.
[28]F. Sattin, "A semiclassical over-barrier model for charge exchange between highly charged ions and one-optical-electron atoms," J. Phys. B: At., Mol. Opt. Phys. **33**, 861–867 (2000).
[29]F. Sattin, "Classical overbarrier model to compute charge exchange and ionization between ions and one-optical-electron atoms," Phys. Rev. A **62**, 042711-1–042711-10 (2000).
[30]F. Sattin, "Further study of the over-barrier model to compute charge-exchange processes," Phys. Rev. A **64**, 034704-1–034704-4 (2001).
[31]T. Ohyama-Yamaguchi and A. Ichimura, "A three-center over-barrier model with screening for multiple ionization of rare gas dimers by slow highly charged ions," Phys. Scr. **T144**, 014028-1–014028-3 (2011).
[32]V. N. Ostrovsky, "Rydberg atom-ion collisions: Classical overbarrier model for charge exchange," J. Phys. B: At., Mol. Opt. Phys. **28**, 3901–3914 (1995).
[33]A. Niehaus, "A classical model for multiple-electron capture in slow collisions of highly charged ions with atoms," J. Phys. B: At., Mol. Opt. Phys. **19**, 2925–2937 (1986).
[34]J. Lindhard and M. Scharff, "Energy dissipation by ions in the kev region," Phys. Rev. **124**, 128–130 (1961).
[35]W. Kohn and L. J. Sham, "Self-consisten equations including exchange and correlation effects," Phys. Rev. **140**, A1133–A1138 (1965).
[36]A. K. Rajagopal and J. Callaway, "Inhomogeneous electron gas," Phys. Rev. B **7**, 1912–1919 (1973).
[37]R. Ritter, R. A. Wilhelm, M. Stögerpollach, R. Heller, A. Mücklich, U. Werner, H. Vieker, A. Beyer, S. Facsko, and A. Gölzhäuser, "Fabrication of nanopores in 1 nm thick carbon nanomembranes with slow highly charged ions," Appl. Phys. Lett. **102**, 770–776 (2013).